



**HAL**  
open science

# Is soil contamination a missing driver of soil heterotrophic respiration in land surface models? A study case with copper –

Laura Sereni, Isabelle Lamy, Bertrand Guenet

## ► To cite this version:

Laura Sereni, Isabelle Lamy, Bertrand Guenet. Is soil contamination a missing driver of soil heterotrophic respiration in land surface models? A study case with copper –. *Science of the Total Environment*, 2024, 957, 10.1016/j.scitotenv.2024.177574 . hal-04795025

**HAL Id: hal-04795025**

**<https://ens.hal.science/hal-04795025v1>**

Submitted on 21 Nov 2024

**HAL** is a multi-disciplinary open access archive for the deposit and dissemination of scientific research documents, whether they are published or not. The documents may come from teaching and research institutions in France or abroad, or from public or private research centers.

L'archive ouverte pluridisciplinaire **HAL**, est destinée au dépôt et à la diffusion de documents scientifiques de niveau recherche, publiés ou non, émanant des établissements d'enseignement et de recherche français ou étrangers, des laboratoires publics ou privés.



# Is soil contamination a missing driver of soil heterotrophic respiration in land surface models? A study case with copper –

Laura Sereni<sup>a,\*</sup>, Isabelle Lamy<sup>a</sup>, Bertrand Guenet<sup>b</sup>

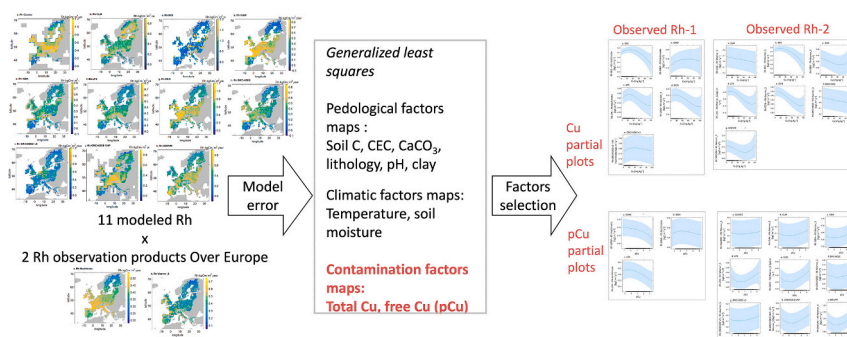
<sup>a</sup> Université Paris-Saclay, INRAE, AgroParisTech, UMR EcoSys, 91120 Palaiseau, France

<sup>b</sup> Laboratoire de Géologie ENS, PSL Research University, CNRS, UMR 8538, IPSL, Paris, France

## HIGHLIGHTS

- Soil contamination affects microbial processes and is widely spread.
- Biases of land surface model's heterotrophic respiration are not fully understood.
- We hypothesized that soil contamination might be a missing driver.
- 11 land surfaces models residuals were analyzed against soil Cu contamination.
- Total and free Cu in soils explain partially some of the models biases.

## GRAPHICAL ABSTRACT



## ARTICLE INFO

Editor: Paulo Pereira

### Keywords:

Land carbon fluxes  
Contaminant availability  
Regional land surface model  
Model comparisons

## ABSTRACT

Land Surface Models (LSMs) are crucial elements of Earth System Models used to estimate the effects of anthropogenic greenhouse gas (GHG) emissions on Earth's climate. Nevertheless, as well as land use change and direct GHG emissions, anthropogenic activities are also associated with contaminant emissions and depositions. Although contamination has a recognized impact on soil processes such as GHG emissions, soil contamination is currently not considered as an important process to consider into LSMs.

In this study we hypothesized that soil contamination has significant impact on soil CO<sub>2</sub> emissions such as heterotrophic respiration (Rh). To this end, we analyzed how soil contamination may account for residuals of modeled Rh from 11 LSMs as compared to Rh products derived from observations over Europe. We used generalized least squared mixed models to evaluate the primary factors driving of the model residuals. Among contaminants, we focused on copper (Cu), which is widely used in industry or agriculture, causing significant diffuse contamination. Additionally, research demonstrated a strong correlation between soil Rh and Cu availability to soil fauna and various soil pedological and climatic parameters. Hence, we completed our analysis by including pedo-environmental parameters and by analyzing Rh against a proxy of bioavailable Cu.

\* Corresponding author at: Université Paris-Saclay, INRAE, AgroParisTech, UMR EcoSys, 91120 Palaiseau, France.

E-mail address: [laurasereni@yahoo.fr](mailto:laurasereni@yahoo.fr) (L. Sereni).

<sup>1</sup> Present address: Univ. Grenoble Alpes, CNRS, INRAE, IRD, Grenoble INP, IGE, Grenoble, France.

<https://doi.org/10.1016/j.scitotenv.2024.177574>

Received 21 May 2024; Received in revised form 1 November 2024; Accepted 13 November 2024

Available online 20 November 2024

0048-9697/© 2024 The Authors. Published by Elsevier B.V. This is an open access article under the CC BY license (<http://creativecommons.org/licenses/by/4.0/>).

Our findings indicate that Cu is a non-negligible variable in explaining the Rh models inaccuracy considering either total or free Cu forms. Therefore, it can be concluded that Cu should not be disregarded as a key factor in predicting Rh.

## 1. Introduction

Land surface models (LSMs) are used within Earth Systems Models since the 1970s to predict climate based on physical atmospheric and oceanographic models (Fisher and Koven, 2020). For years they've been acknowledged as beneficial and improved by several components such as the continental biogeochemical cycle which considered the large fluxes of carbon (C) (and more recently nitrous) between soils and atmosphere (Cox et al., 2000; Friedlingstein et al., 2006; Vuichard et al., 2019; Zaehle and Friend, 2010). However, even with improvements made over last decades there are still uncertainties in modelling some of the major processes. For instance, soil C stocks represents 1500 PgC and C fluxes between the soils and the atmosphere are on the order of 90 PgC year<sup>-1</sup> (Hashimoto et al., 2015). Anav et al. (2013) estimated that only 6 over the 15 tested Earth system models correctly reproduce the land carbon sink, and that all models underestimated C sink from 200 to 50 % in the Northern Hemisphere.

Up to now models of soil C fluxes are mostly governed by soil temperature, soil moisture, clay content, the amount of soil organic carbon and the C input to the soil from primary production (Blyth et al., 2021; Fisher and Koven, 2020). However, increasing human influence not only impacts greenhouse gases (GHG) emissions but also significantly alters soil contamination. For instance, industrial activities, urban traffic, or agriculture may raise the concentration of contaminants in soil, such as heavy metals or pesticides which can in turn impact soil functions (Bååth, 1989; Cao et al., 1984; Steinnes et al., 1997; Yang et al., 2006). Furthermore, soil contamination is predicted to fluctuate over the next decades, mainly contingent on international or local policies (Ballabio et al., 2018; Panagos et al., 2018). Thus, if soil contamination affects soil GHG emissions, it is crucial to incorporate it into account into LSMs to 1) adjust the scenario of climate change under the current contamination and 2) acknowledge the impact of contamination on GHG emissions and climate change when exploring land use change scenarios or defining contamination guidelines. Among land-atmosphere fluxes, soil heterotrophic respiration (Rh) accounts for approximately 40–50 PgC·yr<sup>-1</sup> (Konings et al., 2019; Yao et al., 2021), while soil contamination has been found to affect soil's microbes at the origin of Rh (Giller et al., 2009, 1998; Sereni et al., 2021).

Among pollutants, Cu is widely used in industry or in agriculture through fertilizers and pesticides which introduce contamination that adds to soil natural background concentrations. These concentrations vary from 5 to 50 mg Cu kg<sup>-1</sup> soil as a result of the different parent materials (Thornton and Webb, 1980) while concentrations up to 150 mg Cu kg<sup>-1</sup> in vineyards or even 3000 mg Cu kg<sup>-1</sup> close to industries can be found (Ballabio et al., 2018; Smorkalov and Vorobeichik, 2011). Due to the major use of Cu in different agricultural practices, its application is strongly regulated at the European scale (Official Journal of the European Union, 2018). Nevertheless, it has been reported that the accumulation of Cu in soils are closely linked to soil factors like such as pH, clay, CaCO<sub>3</sub> or organic matter contents (Ballabio et al., 2018). Furthermore, it has been demonstrated that soil Cu concentrations significantly impact soil CO<sub>2</sub> emissions in diverse contamination scenarios such as laboratory spikes, industrial or agricultural fields, forests, etc. (Giller et al., 2009; Sereni et al., 2021). Besides, Cu have been studied since a long time and several data and studies are available on its soil concentration. However, the effect of soil Cu concentrations on field-scale CO<sub>2</sub> emissions remains uncertain.

The effect of soil Cu on GHG emissions is expected to occur through its effects on soil microbes' respiration. However, it is widely accepted that not all the total metal content is biologically available. For instance,

according to the free ion activity model only the small amount of Cu in the form of free ions in the soil solution, called available fraction, may be the only effectively bio-available form that can have an impact on soil fauna (Lanno et al., 2004; Lofts et al., 2013; Parker et al., 2001; Thakali et al., 2006). Cu availability is greatly influenced by soil characteristics such as soil pH or soil organic C, so that available Cu level increases at low pH and low organic matter content (McBride et al., 1997). Therefore, total Cu was sometimes found a suitable proxy to evaluate the effect of soil contamination on soil fauna, but in some cases free Cu should be favored (Pauget et al., 2012).

In this study, our objective was to investigate the errors of continental biogeochemical models in reproducing observation-based products of Rh partially attributable to Cu content. Continental land surface biogeochemical models differ in the mechanisms they simulate and the incorporation of environmental factors. Additionally, models differ in the spatial variations of soil Rh. Models intercomparison is then frequently used to estimate the model's residual patterns and required improvement. It is also used to differentiate between individual misrepresentation and missing first order drivers that require better representation residual (Huntzinger et al., 2017). Thus, we used models output from the TRENDY database (Sitch et al., 2015) to investigate the hypothesis that soil Cu concentrations, as an additional environmental variable, affect the models' residuals. Because direct observations of Rh fluxes on a large scale are seldom, we used two different products of observation, hypothesizing that bias of importance varied between both products. We investigated both the effects of total Cu and the effect of free Cu (considered here as bioavailable) on soil CO<sub>2</sub> emissions. However, available databases containing information suitable for large scale only recorded total Cu as it is a simpler measurement to obtain than free Cu (Ballabio et al., 2018; Tóth et al., 2016). Among the numerous empirical existing equations to derive bioavailable Cu, we chose the Tipping et al. (2003) estimation which is one of the most used transfer functions based on >90 observations. This equation coupled with the data on soil properties provided by the JRC enable estimation of free Cu at the EU Level.

## 2. Materials and methods

### 2.1. Sources of soil data

Data of soil total Cu, soil organic C (SOC), soil pH, soil clay percentage, soil cationic exchange capacity (CEC) and soil CaCO<sub>3</sub> content were downloaded from the JRC data files. References can respectively be found in Ballabio et al. (2018) for total Cu, de Brogniez et al. (2015) for SOC, Ballabio et al. (2016) for clay and Ballabio et al. (2019) for CaCO<sub>3</sub> and CEC values. Samples were collected at approximately 14 \* 14 km intervals across the 0–20 cm horizons. The initial Cu data ranged from 0 to 496.3 mg·kg<sup>-1</sup> with a high variability (mean 16.9 mg kg<sup>-1</sup>, standard deviation is 21.9 mg kg<sup>-1</sup>). The correlations between variables are presented in supplementary Fig. S1. Statistical correlations have been well described in Ballabio et al. (2018) including correlation with land use and geographical administrative regions has been well described. The regridded Cu data range from 2.0 to 103.1 mg kg<sup>-1</sup> with mean 15.7 mg kg<sup>-1</sup> and standard deviation at 10.3 mg kg<sup>-1</sup>.

Net Primary Production (NPP) observations used are the products provided by (Smith et al., 2016). This product relies on the Moderate Resolution Imaging Spectroradiometer NPP algorithm, driven by long-term Global Inventory Modelling and Mapping Studies (GIMMS) fraction of photosynthetically active radiation and leaf area index data, to compute a 30-year worldwide data set of satellite-derived NPP

(1982–2011).

It was hypothesized that soil Cu concentration had remain relatively stable in recent decades. As a result, the data provided by the JRC in 2015 was used for comparison over the 1982–2010-time span. The concentration of free Cu was computed as proxy of bio available Cu (Parker et al., 2001). Free ion  $\text{Cu}^{2+}$  concentration was expressed as  $\text{pCu} = -\log(\text{Cu}^{2+})$  with the Eq. (1) from Tipping et al. (2003):

$$\text{pCu} = 1.17 \text{ pH} - 1.09 \log_{10}\text{Cu} + 0.52 \log_{10}(2\text{xSOC}) - 5.35 \quad (1)$$

Co-variables used to calculate free Cu were from the JRC databases (Ballabio et al., 2019; de Brogniez et al., 2015). The correlations between  $\text{pCu}$  and others variables are presented in Fig. S2.

The data were collected at a scale of 0.5 km and regridded to a resolution of  $0.5^\circ$  using the climate data operator cdo at  $0.5^\circ$  to fit with the TRENDY models' resolution.

## 2.2. Observations of heterotrophic respiration data

Two products of observation for Rh were used for comparison: one was provided by Hashimoto as yearly means over the 1901–2010 period and at the  $0.5^\circ$  scale (Hashimoto et al., 2015). Most of the observations were conducted after 1990. Hashimoto's product is based on a semi-empirical approach that defines Rh responses to temperature and rainfall based on observations. The product then estimates Rh at a global scale on the based on climatic measurements. These observations-based product will be further named Rh Hashimoto. The other observations-based product of Rh is provided by Warner as mean of the 1961–2010 period at a 1 km scale (Warner et al., 2019). These observations product was generated using machine learning trained on more than two thousand observations that data base provides. The soil respiration fluxes and two Rh fluxes derived from it are provided in Warner et al. (2019). Since both derivations are linear products of the same co-factors, we only use the estimation of heterotrophic respiration from the Subke derivation (further referred to as Rh Warner\_S). These observations were regridded at  $0.5^\circ$  to fit with the TRENDY simulation resolution. None of these two databases is a direct observation of Rh but statistical estimate of worldwide Rh based on punctual measurements. However, the derivations methods being very different their combine use allows a much stronger estimation of Rh.

## 2.3. Model respiration data

The TRENDY-v9 project (Sitch et al., 2015) provides the land component of the Global Carbon Project 2020 Budget with a collection of land carbon simulations provided by and accessible for a consortium of dynamic global vegetation model DGVM groups. Models are forced over the 1700–2019 period with changing  $\text{CO}_2$ , climate and land use according to the S3 protocol detailed in <https://sites.exeter.ac.uk/trendy> (last accessed on 17 September 2021). Briefly, the models are forced over 1901–2019 using the monthly or 6 h historical forcing data from Climate Research Units (CRU) provided by Ian Harris at UEA 1901–2019 and accessible at [https://crudata.uea.ac.uk/cru/data/hrg/cru\\_ts.4.04/](https://crudata.uea.ac.uk/cru/data/hrg/cru_ts.4.04/) (Mitchell et al., 2004). Atmospheric  $\text{CO}_2$  data for the 1700–2019 time period are derived from ice core  $\text{CO}_2$  data combined with national oceanic and atmospheric administration (NOAA) data from 1958 onwards. Land Use change data is derived from updated information contained within the History Database of the global Environment (HYDE) for the years 1960–2020 alongside recent wood harvest data from the food and agriculture organization of the united nation (FAO). The Trendy-v9 database provides results for 20 models with variable data presented in separate netcdf files. Files from the same model were combined into a single netcdf file at a resolution of  $0.5^\circ$  and aggregated into yearly data for the period 1900–2019. Finally, an average was calculated over the period 1980–2011. Models with coarser resolution were removed from the comparison.

Because Rh is strongly correlated with NPP, soil moisture, air

temperature and soil SOC content we aimed at including these variables from the models before comparison with observations. Also, we excluded models from the entire TRENDY database that lacked one of these variables. This led to a total of 11 models: CLASSIC (Canadian Land Surface Scheme including Biogeochemical Cycle (Melton et al., 2020; Seiler et al., 2021)), CLM (Community Land Surface Model (Lawrence et al., 2019)), IBIS (Integrated Biosphere Simulator (Yuan et al., 2020)), ISAM (Integrated Science Assessment Model (Meiyappan et al., 2015)), ISBA (Interaction Soil-Biosphere-Atmosphere (Delire et al., 2020)), LPX (Land Surface Processes eXchanges (Lienert and Joos, 2018)), OCN (ORCHIDEE C N (Zaehle and Friend, 2010)), ORCHIDEE (Organising Carbon and Hydrology In Dynamic Ecosystems (Krinner et al., 2005)), ORCHIDEE v3 (Vuichard et al., 2019), ORCHIDEE CNP (Goll et al., 2017) and SDGVM (Sheffield Dynamic Global Vegetation Model (Walker et al., 2017)).

## 2.4. Statistical analysis

We investigated the disparities between Rh estimated by each model and each Rh from observation-based products. To identify the drivers of the model residuals we used two different sets of predictors. One set consider total Cu and then included: clay, CEC, pH, total Cu, temperature, soil moisture, the differences between NPP ( $\Delta\text{NPP}$ , Eq. (2)),  $\text{CaCO}_3$  and the differences between SOC ( $\Delta\text{SOC}$ , Eq. (3)) and is named set T (for total Cu). The second set consider free Cu and then included: clay, CEC, free Cu (considered as a proxy for bioavailable Cu and defined based on Eq. (1)), temperature, soil moisture, the differences of NPP ( $\Delta\text{NPP}$ , Eq. (2)) and  $\text{CaCO}_3$  and is named set F (for free Cu).

$$\Delta\text{NPP}_i = \text{NPP}_i - \text{NPP observed} \quad (2)$$

$$\Delta\text{SOC}_i = \text{SOC}_i - \text{SOC observed} \quad (3)$$

With  $i$  being a trendy model, NPP observed and SOC observed being dataset described in Section 2.1.

When looking for second order processes, classical models such as linear mixed-effect model were not relevant because we hypothesized threshold in Cu effect and because neither raw nor log transformed variables exhibited normal distribution. Also, we hypothesized that our covariables were spatially correlated. Therefore, we adopted a two-fold methodology. First, we compared several linear generalized least-square models with no or different spatial structures (Gaussian, exponential, spherical, linear or rational (using the gls package (Pinheiro et al., 2023)). Based on AIC values we selected exponential spatial correlations with the smallest AIC values for the following analysis. In a second step, we used polynomial generalized least square estimations (gls, package) with all terms represented at their 3rd degree and exponential spatial correlation. The use of this method allows us to account for the spatial correlation between the different variables. In some cases (CLM, CLASSIC, ISAM, OCN, ORCHIDEE CNP, SDGVM for comparison with set T of predictors and for comparison with set F of predictors and Warner\_S's Rh and for all except ORCHIDEE v3 with set F of predictors and Hashimoto's Rh), we implemented degree 2 instead of degree 3 for CEC and  $\text{CaCO}_3$  predictors to ensure convergence of the model. We used the stepAIC function to select variables for the final model, aiming to maintain the most parsimonious model based on the AIC criteria. All statistical analysis were conducted using R v3.5 (R Core Team, 2018). Finally, as the Cu maps provided by the JRC are generated at the EU-scale, all the analyses were performed over the EU region.

## 3. Results

### 3.1. Observed heterotrophic respiration fluxes

The maps of mean Rh fluxes period for Europe are shown in Fig. S3 for both Hashimoto (a) and Warner\_S (b) observations-derived products. Hashimoto Rh's fluxes were about  $0.36 \pm 0.06 \text{ kgC m}^{-2} \text{ y}^{-1}$  (mean, sd)

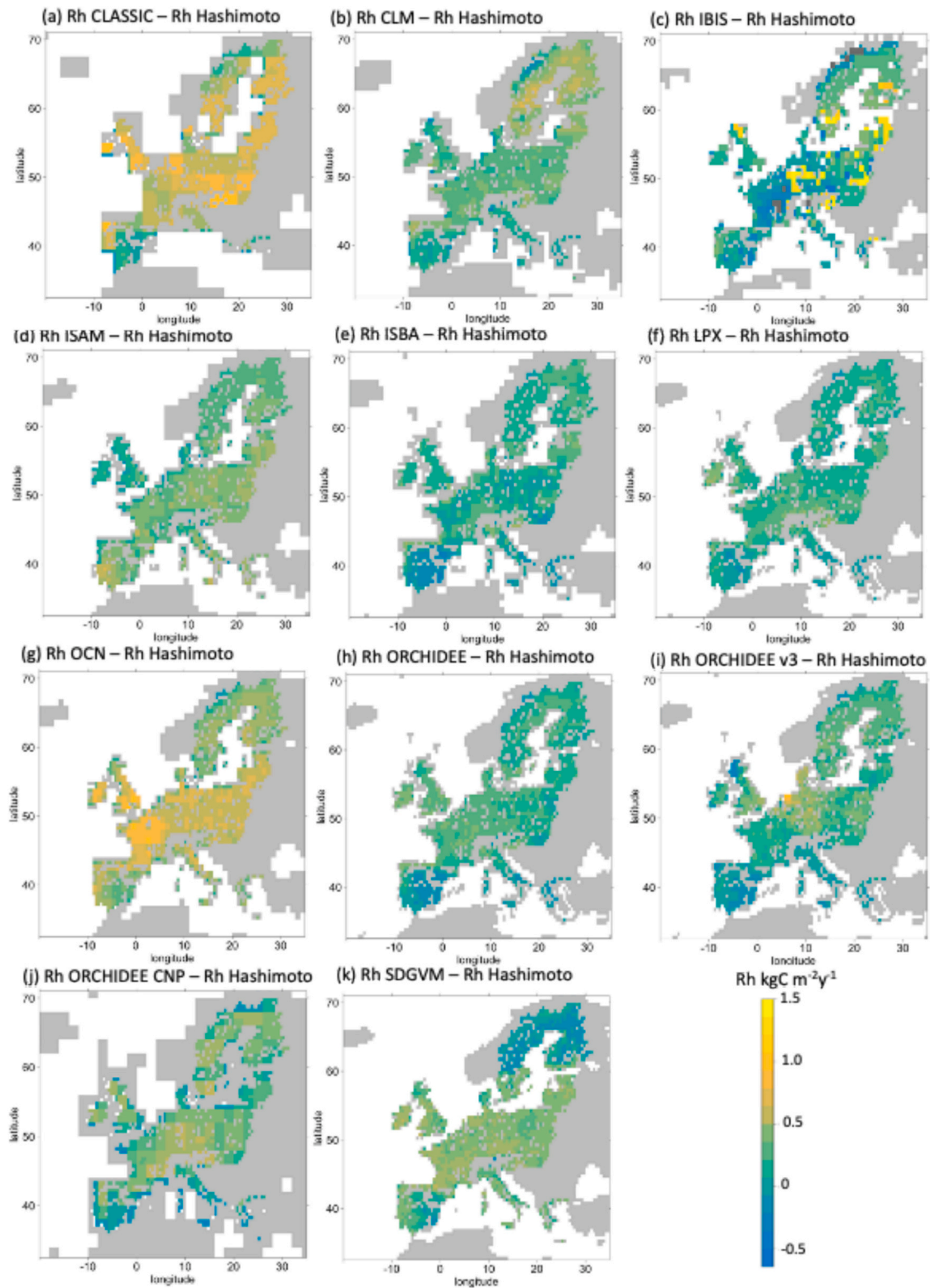


**Fig. 1.** Differences of heterotrophic respiration (Rh) fluxes between the different LSM models and Hashimoto's Rh in  $\text{kgC m}^{-2} \text{year}^{-1}$  (a) CLASSIC model, (b) CLM model, (c) IBIS model, (d) ISAM model, (e) ISBA model, (f) LPX model, (g) OCN model, (h) ORCHIDEE model, (i) ORCHIDEE v3 model, (j) ORCHIDEE CNP model and (k) SDGVM model filtered over the EU territory. Grid points in light grey are for zone without SOC data, for IBIS dark grey grid points correspond to negatives Rh values and were removed.

with a minimum of 0.26 and maximum of 0.54 whereas Warner\_S Rh's fluxes were about  $0.34 \pm 0.01 \text{kgC m}^{-2} \text{y}^{-1}$  (mean, sd) but varied from 0.07 to 0.66  $\text{kgC m}^{-2} \text{y}^{-1}$  (Table S1). The Rh Warner\_S also showed variations in Rh at a finer scale than the observation of Hashimoto. In

both instances Rh fluxes increased from the south-west to the north-east of Europe. However, Rh Warner\_S displayed more scattered patterns with more isolated variations. For instance, with Rh Warner\_S, Croatia and North-West of Italy presented higher fluxes than the South of Alps,

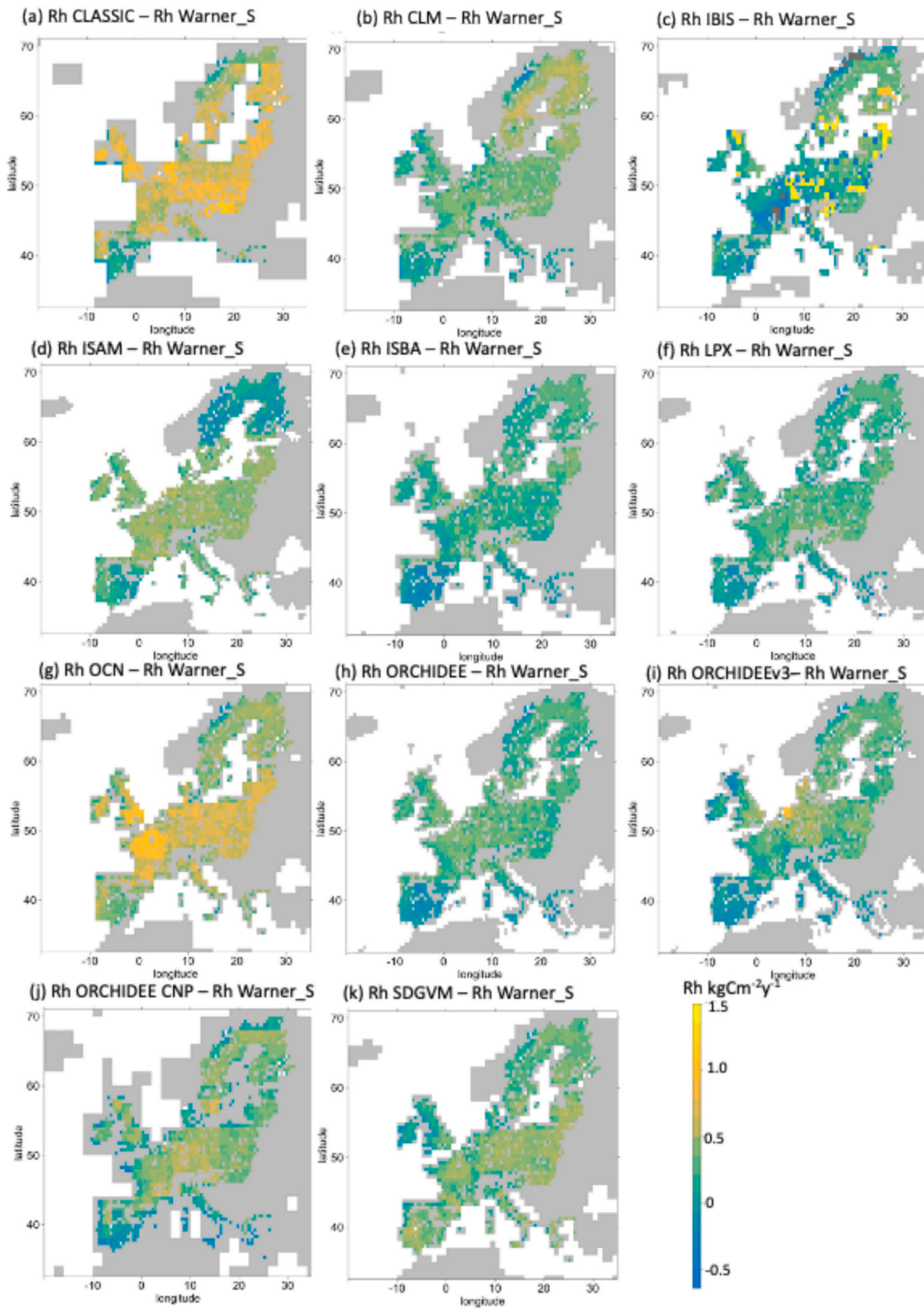


**Fig. 2.** Differences of heterotrophic respiration (Rh) fluxes between the different LSM models and Warner\_S's Rh in  $\text{kgC m}^{-2} \text{year}^{-1}$ . (a) CLASSIC model, (b) CLM model, (c) IBIS model, (d) ISAM model, (e) ISBA model, (f) LPX model, (g) OCN model, (h) ORCHIDEE model, (i) ORCHIDEE v3 model, (j) ORCHIDEE CNP model and (k) SDGVM model filtered over the EU territory. Grid points in light grey are for zone without SOC data, for IBIS dark grey grid points correspond to negatives Rh values and were removed.

**Table 1**

Predictors selected by the step AIC procedure to explain differences between modeled and observed Rh with the T set of predictors in initial gls model. Crosses indicate that a predictor (column) has been selected as significant to explain difference between modeled Rh (row) and observed Rh. Residual standard error of the final model are indicated. For CLM and ORCHIDEE the comparison with Rh Hashimoto's was made with the mean over 1990–2019 as gls didn't converged using the 1980–2010 mean. Corresponding partial plots are presented in Figs. S5 to S15 for Rh Hashimoto and Figs. S16 to S26 for Rh Warner\_S (a): with Rh Hashimoto for comparison (b); with Rh Warner\_S for comparison; (c) is the number of times where each predictor is conserved over (a) and (b) Number of models tested are indicated in the parentheses in the first column.

(a)											
Rh Model-Rh Hashimoto	Lithology	Soil moisture	Temperature	$\Delta$ SOC	$\Delta$ NPP	Cu	pH	Clay	CEC	CaCO <sub>3</sub>	Residual error
CLASSIC		X	X		X		X			X	0.45
CLM (90-19)		X	X	X	X				X		0.2
ISAM		X	X	X	X	X	X	X	X		0.1
ISBA		X	X	X	X		X	X			0.1
IBIS		X	X	X	X	X	X	X	X		0.22
LPX		X	X	X	X	X	X	X			0.06
OCN		X	X	X	X	X	X				0.12
ORCHIDEE (90-19)		X	X	X			X	X			0.09
ORCHIDEE V3		X	X	X	X	X		X			0.16
ORCHIDEE CNP		X	X	X	X		X		X		0.19
SDGVM		X	X	X	X				X		0.16
(b)											
Rh Model-Rh Warner_S	Lithology	Soil moisture	Temperature	$\Delta$ SOC	$\Delta$ NPP	Cu	pH	Clay	CEC	CaCO <sub>3</sub>	Residual error
CLASSIC			X	X	X		X	X		X	0.42
CLM		X	X	X	X	X	X		X		0.22
ISAM		X	X	X	X			X	X		0.11
ISBA		X	X	X		X	X	X		X	0.12
IBIS		X	X	X	X	X	X	X	X		0.23
LPX			X	X	X	X		X		X	0.09
OCN		X	X	X	X	X	X	X			0.13
ORCHIDEE		X	X	X		X		X		X	0.16
ORCHIDEE V3		X	X	X	X		X	X			0.22
ORCHIDEE CNP											
SDGVM		X	X	X	X	X	X	X			0.13
(c)											
	Lithology	Soil moisture	Temperature	$\Delta$ SOC	$\Delta$ NPP	Cu	pH	Clay	CEC	CaCO <sub>3</sub>	
Occurrence Model – Rh Hashimoto's (/11)	0	11	11	11	10	5	8	6	5	1	
Occurrence Model – Rh Warner's (/11)	0	9	11	10	9	7	8	10	4	5	
Sum Occurrence (/22)	0	20	22	21	18	12	16	16	9	6	

whereas with Hashimoto's database the entire Alpine region exhibited similar fluxes.

### 3.2. Modeled heterotrophic respiration fluxes at the European scale

Minimum, maximum, median, 1st and 3rd quartile and mean Rh fluxes of the 11 models are presented in Table S1. The mean Rh fluxes value across the 11 models is  $0.35 \text{ kgC m}^{-2} \text{ y}^{-1}$  (standard deviation = 0.24). The median is 0.34, the maximum is 1.75 and the minimum is 0. Most of the highest respiration fluxes are modeled by CLASSIC and OCN (CLASSIC median Rh  $0.79 \text{ kgC m}^{-2} \text{ y}^{-1}$  and 3rd quartile  $0.85 \text{ kgC m}^{-2} \text{ y}^{-1}$ , OCN median Rh  $0.75 \text{ kgC m}^{-2} \text{ y}^{-1}$  and 3rd quartile  $0.82 \text{ kgC m}^{-2} \text{ y}^{-1}$ ). However, the maximum value is obtained with IBIS ( $1.75 \text{ kgC m}^{-2} \text{ y}^{-1}$ ). The modeled Rh fluxes at the EU scale are shown in Fig. S4. Most of the models reproduce the North-East gradient of increase in Rh fluxes and the decrease in Scandinavia but the respective spatial extent differs. For instance, ISAM and OCN show a high contrast between Scandinavia and Spain Rh fluxes. By contrast, ORCHIDEE v3 or IBIS show a light gradient but particularly high respiration levels in Germany.

### 3.3. Residuals of modeled Rh

Minimum, maximum, 1st and 3rd quartile, mean and median values for  $\Delta$ Rh between each model and Hashimoto's Rh and between each

model and Warner\_S's Rh are presented respectively in Tables S2a and S2b. Over the studied area, we observed a widespread overestimation of Rh fluxes with median and mean values for the differences between all model and observed Rh  $> 0$  (respectively mean =  $0.08 \text{ kgC m}^{-2} \text{ y}^{-1}$  and median =  $0.05 \text{ kgC m}^{-2} \text{ y}^{-1}$  when compared with the Hashimoto's Rh products and mean =  $0.10 \text{ kgC m}^{-2} \text{ y}^{-1}$ , median =  $0.08 \text{ kgC m}^{-2} \text{ y}^{-1}$  when compared to Warner\_S's products). When compared to the Hashimoto's Rh products, 4 of the 11 models (ISBA, IBIS, ORCHIDEE and ORCHIDEE v3) underestimate Rh for more than half of the grid points (median difference of Rh and Rh Hashimoto  $< 0$  for all these models). When compared to the Warner\_S's product only IBIS model underestimates Rh for more than half of the grid points, see Table S2.

Differences between modeled Rh and Hashimoto's Rh are presented in Fig. 1, while Fig. 2 presents the differences between modeled Rh and Warner\_S's Rh product. The comparison of each model to each observation product displays a global increase in overestimation towards the North-Eastern area and in some cases in Spain or Italy (Classic, CLM, OCN or ORCHIDEE vs Hashimoto's Rh and to a lesser extent vs Warner\_S observations products). Finally, if the models reproduce the global Rh's spatial, the magnitude is globally overestimated.

### 3.4. Statistical models to explain modeled Rh residuals

#### 3.4.1. Effect of pedo-climatic predictors to explain modeled Rh residuals

The residuals of Rh (difference between model and observed Rh) for

**Table 2**

Predictors selected by the step AIC procedure to explain differences between modeled and observed Rh with the F set of predictors in initial gls model. Crosses indicate that a predictor (column) has been selected as significant to explain differences between modeled Rh (row) and observed Rh. Residuals standard errors of the final model are indicated. For CLM and ORCHIDEE comparisons with Hashimoto's Rh gls did not converged neither with the 1980–2010 nor with the 1990–2019 means. Corresponding partial plots are presented in Figs. S27 to S35 for Rh Hashimoto and in Figs. S36 to S46 for Warner\_S's Rh (a): with Hashimoto's Rh for comparison (b); with Warner\_S's Rh for comparison. (c). is the number of times where each predictor is conserved over (a) and (b) Number of models tested are indicated in the parentheses in the first column.

(a)	Lithology	Soil moisture	Temperature	pCu	Clay	$\Delta$ NPP	CEC	CaCO <sub>3</sub>	Residual error
CLASSIC		X	X			X			0.43
CLM	–	–	–	–	–	–	–	–	–
ISAM		X	X	X		X	X		0.11
ISBA		X	X	X	X	X			0.1
IBIS		X	X						0.33
LPX		X	X	X	X	X	X		0.07
OCN		X	X			X			0.12
ORCHIDEE	–	–	–	–	–	–	–	–	–
ORCHIDEE V3		X	X			X			0.16
ORCHIDEE CNP		X	X			X			0.22
SDGVM		X	X			X	X		0.17

(b)	Lithology	Soil moisture	Temperature	pCu	Clay	$\Delta$ NPP	CEC	CaCO <sub>3</sub>	Residual error
CLASSIC			X	X		X			0.43
CLM		X	X	X	X	X	X		0.22
ISAM		X	X		X	X	X		0.11
ISBA		X	X	X	X			X	0.12
IBIS		X	X			X			0.32
LPX			X	X	X	X		X	0.09
OCN		X	X	X	X	X			0.14
ORCHIDEE		X	X	X	X			X	0.16
ORCHIDEE V3		X	X	X	X	X			0.22
OCRCH CNP		X	X	X	X	X			0.19
SDGVM		X	X	X	X	X			0.13

(c)	Lithology	Soil moisture	Temperature	pCu	Clay	$\Delta$ NPP	CEC	CaCO <sub>3</sub>
Occurrence Model – Rh Hashimoto's (/9)	0	9	9	3	2	8	3	0
Occurrence Model – Rh Warner'S (/11)	0	9	11	9	9	9	2	3
Sum Occurrence (/20)	0	18	20	12	11	17	5	3

the different models were analyzed against several driving factors (see Section 2.4). After variable selections through stepAIC the mean residual error for heterotrophic respiration of the statistical models were found to be  $0.17 \pm 0.10$  (set T) and  $0.19 \pm 0.12$  (set F) when compared to Hashimoto's Rh. When compared with Warner\_S's Rh, statistical models' residual error was found to be  $0.18 \pm 0.09$  (set T) and  $0.19 \pm 0.10$  (set F). The  $\Delta$ Rhs were better captured by the statistical model for LPX (smallest residual standard error) but not for CLASSIC (largest residual standard error, see Table 1) for the comparison to both Hashimoto and Warner\_S's Rh. The terms conserved by the stepAIC selection and Rh are respectively displayed in Tables 1a, 2a for the comparison with Hashimoto's Rh and 1b, 2b for the comparison with Warner\_S's Rh. These terms selection consider set T (Table 1) or set F (Table 2) of initial predictors. The partial plots showing the selected terms are presented in Figs. S5 to 46 for successively set T and set F of predictors as well as Hashimoto's Rh and Warner\_S's Rh. Figs. S5 to S15 (Hashimoto's Rh) and 16–26 (Warner\_S's Rh) illustrate the selected terms for set T of predictors. Figs. S27 to S35 (Hashimoto's Rh) and S36 to S46 (Warner\_S's Rh) illustrate the selected terms for set F of predictors.

Soil moisture and air surface temperature (as well than  $\Delta$ SOC in the case of set T of initial predictors) were conserved by the stepAIC selection for all the models when Hashimoto's Rh was used for comparison (Tables 1a, 2a). Similarly, the  $\Delta$ NPP was selected as an explanatory variable for all models except for ORCHIDEE models using the set T of initial predictors, and for all models except for IBIS model using the set F

of initial predictors.

Air surface temperature was conserved for all models (Tables 1c, 2c). Soil moisture was conserved for all models except for LPX and CLASSIC models with set T of initial predictors and for all models with set F of initial predictors using Warner\_S's Rh for comparison.  $\Delta$ SOC was conserved for all models except for the ISBA model with set T of initial predictors and Warner\_S's Rh. When compared to Warner\_S's Rh, the  $\Delta$ NPP was also selected as an explanatory variable for all models except for the ORCHIDEE and ISBA models using both set T and F of predictors.

Soil clay was selected in 6/11 cases with the set T of initial predictors and in 2/11 cases with the set F of initial predictors, when using Hashimoto's Rh. By contrast, soil clay was often found to be a significant factor to explain  $\Delta$ Rh with Warner\_S's Rh with selection in 10/11 cases (CLM being excluding) and 9/11 cases (all models except IBIS and CLASSIC) respectively using the sets T and F of initial predictors. StepAIC selection conserved lithology, CEC and CaCO<sub>3</sub> to a lesser extent. Lithology was only found to explain model residuals for two cases (namely ORCHIDEE and CLM) using Hashimoto's Rh for comparison and the set F of initial predictors. CEC was found to be a significant factor in explaining the model residuals in 11 over the 22 studied cases. These cases include the CLM and ISAM models for the two sets of initial predictors and for the two observed Rh. Additionally, for the IBIS and ORCHIDEE CNP models for set T of initial predictors and for the two observed Rh, the SDGVM model for the 2 sets of initial predictors and the LPX model for set F of initial predictors using Hashimoto's Rh

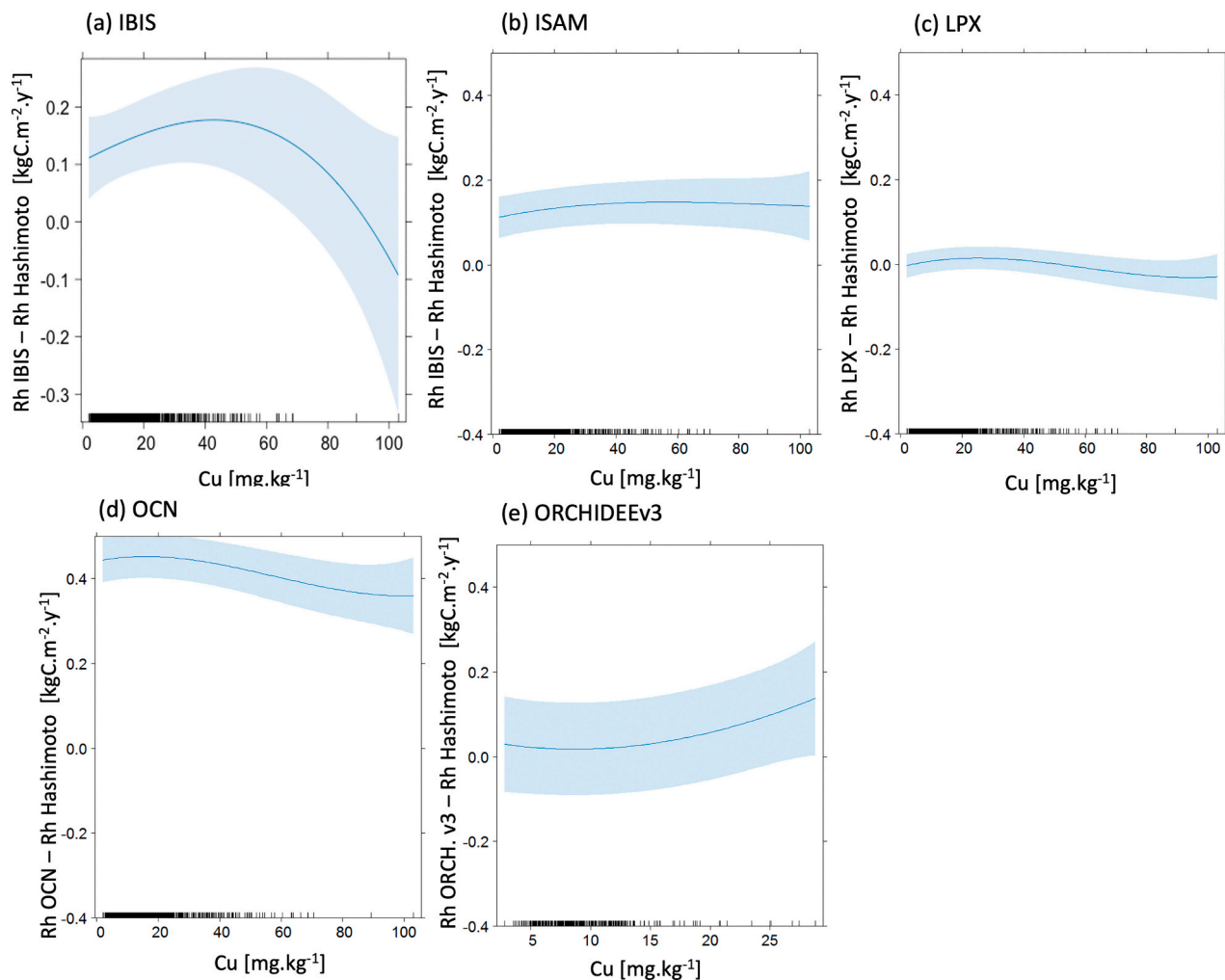


**Fig. 3.** Partial Cu effects plots for the differences between models and Hashimoto's Rh. Results are only shown for models where Cu was selected through step AIC using set T of initial predictors. (a) IBIS model, (b) ISAM model, (c) LPX model, (d) OCN model and (e) ORCHIDEE v3 models.

(Tables 1c and 2c) CEC was found to be significant.  $\text{CaCO}_3$  was preserved solely for the CLASSIC model when using set T of initial predictors and for the ORCHIDEE residuals using set F of initial predictors with Hashimoto's Rh for comparison. When using Warner's Rh,  $\text{CaCO}_3$  was found to be a significant factor to explain Rh residuals for the ISBA, LPX, and ORCHIDEE models with the two sets of initial predictors as well as the CLASSIC and ORCHIDEE CNP models using set T of predictors.

### 3.4.2. Effect of total Cu or bio-available Cu as predictors of modeled Rh residuals

Total Cu was conserved in 12 out of the 22 studied cases by the stepAIC selection and pCu was conserved in 12 out of the 20 studied cases by the stepAIC selection (Tables 1c and 2c respectively). Considering total Cu (set T of initial predictors), Cu was conserved for 5 models (ISAM, IBIS, LPX, OCN and ORCHIDEE v3 models) when Hashimoto's Rh was used for comparison. Cu was conserved more often by the stepAIC selection using Warner's Rh for comparison with selection for 7 models (CLM, ISBA, IBIS, LPX, OCN, ORCHIDEE and SDGVM). When using set F of initial predictors with Hashimoto's Rh for comparison, pCu was conserved three times (ISAM, ISBA and LPX models). By contrast, pCu was conserved 9 times using Warner's Rh (CLM, CLASSIC, ISBA, LPX, OCN, ORCHIDEE, ORCHIDEE v3, ORCHIDEE CNP and SDGVM models).

Thus, for the statistical models constructed through the stepAIC, both Cu and pCu are identified as significant variables as often as soil

moisture and 2–3 times more often than CEC or  $\text{CaCO}_3$ . When pCu (set F) is considered in the initial variables, statistical models are constructed with pCu as many times as clay. Figs. 3 and 4 show the partial effects of total Cu, and Figs. 5 and 6 those of pCu as a predictor of differences between modeled and observed Rh (if Cu or pCu were not conserved into the final statistical model the plots are not shown). When conserved, the partial effect of Cu was found to be of the same order of magnitude ( $10^{-1}$ ) as the other predictors in explaining Rh residuals, except for temperature which had 10 times larger effect (Fig. S5-S44).

Considering the 11 models and the two bases of observations, there is a trend of global decrease in differences between modeled and observed Rh with the increase in soil total Cu. Nevertheless, in certain instances, an increase in differences between modeled and observed Rh was detected for moderate (LPX, IBIS, ISAM) and/or very high Cu concentrations (SDGVM, ISBA but with limited data points).

Finally, the shifts in trends were found to be model dependent and varied depending on the observation products. For instance, considering Rh SDGVM - Rh Warner\_S, the smallest differences occur at a total soil Cu content around  $80 \text{ mgCu.kg}^{-1}$ . Meanwhile, Rh IBIS - Rh Hashimoto consistently exhibits a decline, and the maximum difference between Rh ISAM and Rh Hashimoto is observed around  $50 \text{ mg Cu.kg}^{-1}$  (Figs. 3b, 4b, c).

Results with set F of predictors vary depending on the source of observations. With Hashimoto's Rh, the differences between modeled and observed Rh increase for very small pCu (high free Cu in soil

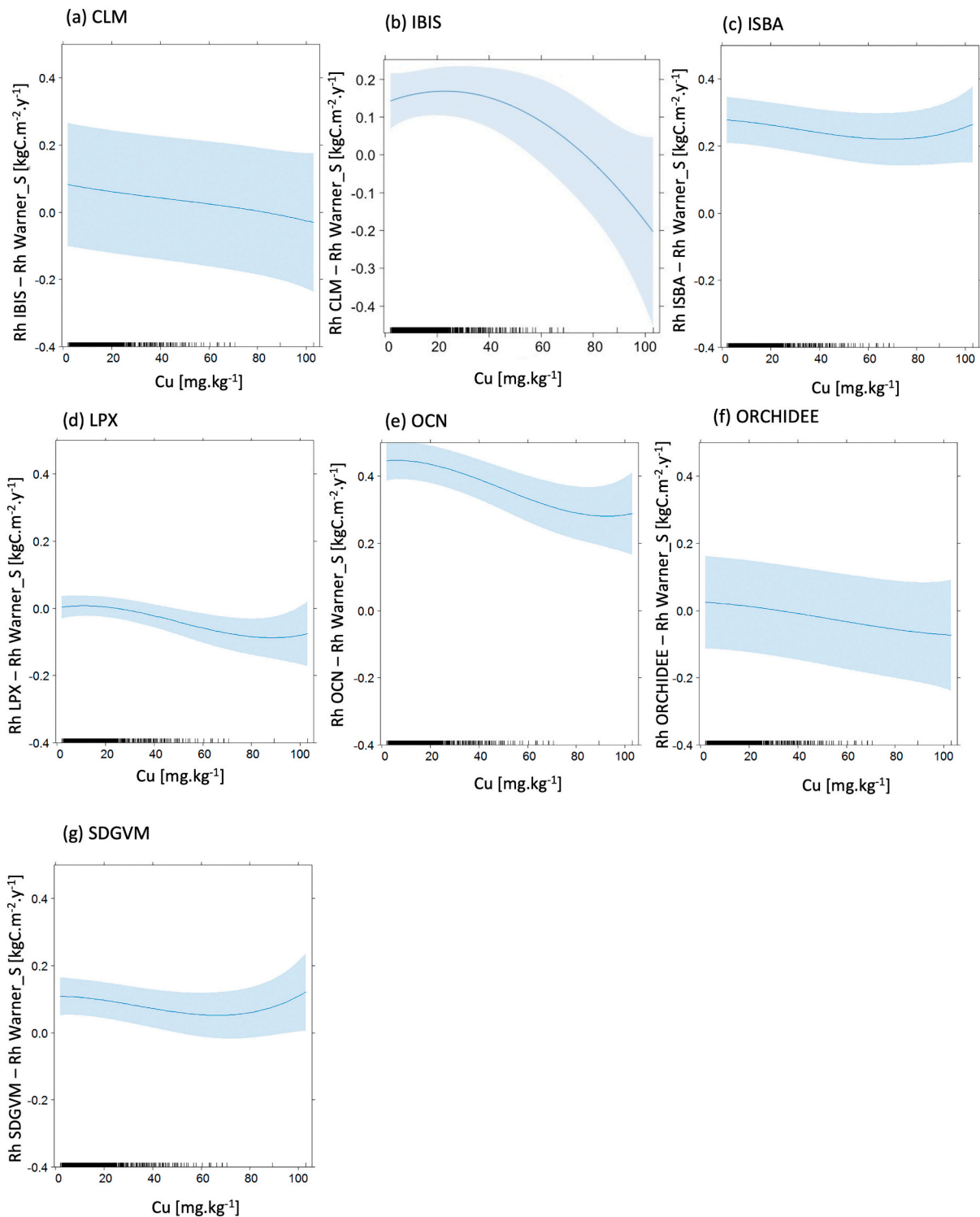


**Fig. 4.** Partial Cu effects plots for the differences between models and Warner\_S's Rh. Results are only show for models where Cu was selected through step AIC using set T of initial predictors. (a) CLM model, (b) IBIS model, (c) ISBA model, (d) LPX model, (e) OCN model, (f) ORCHIDEE model, (g) SDGVM model.

solution) and decrease for high pCu (low free Cu in soil solution), see Fig. 5. By contrast, the differences between modeled Rh and Rh Warner\_S increase for low pCu (high free Cu in soil solution), decrease for moderate pCu and increase for high pCu (low free Cu in soil solution), see Fig. 6.

## 4. Discussion

### 4.1. Integrating soil contamination into LSMs

The present study undoubtedly confirms the necessity of considering the effects of soil moisture, temperature, SOC and NPP in soil Rh modelling. The direct effects of climate and of substrate availability (SOC and NPP) on Rh are well known and numerous attempts are made

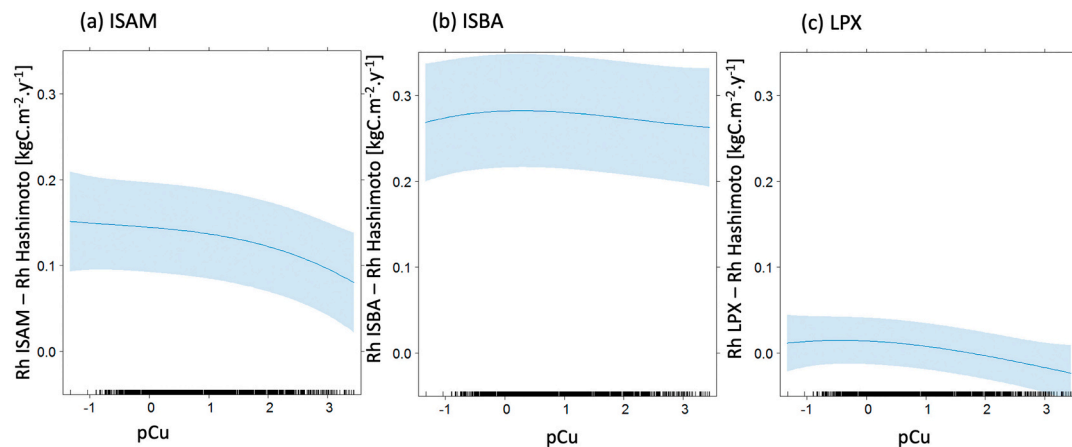


**Fig. 5.** Partial pCu effects plots for the differences between models and Hashimoto's Rh. Results are only shown for models where pCu was selected through step AIC using set F of initial predictors. (a) IBIS model, (b) ISBA model, (c) LPX model.

to precisely account for them in LSMs (Blyth et al., 2021; Vargas et al., 2011). Here, we found that the concentration of soil Cu concentration was also a significant factor to explain differences between modeled Rh and Rh derived from observation products. We observed that in the different models tested against the different dataset used here, Cu was detected as significant explanatory variable as frequently as more traditionally tested variables such as clay, CEC... Moreover, even though lithology has been suggested to be a key factor in explaining soil carbon dynamic (Doetterl et al., 2015), our analysis did not find lithology to be significant. Instead, it appears that Cu may be a more important factor in explaining soil Rh biases in LSMs across Europe. It is noteworthy to note that lithology has been found to be highly correlated with native soil heavy metal contents (Alloway, 2013; Ballabio et al., 2018), which may also be correlated with each other. Nonetheless, the Rh bias of the models was found here to rather results from anthropogenic Cu contamination instead of Cu from the pedological background. Hence, taking soil Cu concentration into account in LSMs may improve their predictive capacities.

Taking into account soil contamination as a novel parameter may be achieved by two approaches: either by defining empirical functions that correct the models based on models' differences to observations products or by establishing mechanistic functions that adjust the modeled component affected by soil contamination.

The first approach requires large databases of chosen endpoints (Rh, NPP, GPP, etc.) and of soil contamination to calibrate the model. The present study illustrates the limitation of this approach, with different results depending on the observation products and the models considered. Additionally, the calibration of statistical functions through observational databases limits the possibility to use the resulting functions for prospective studies. Indeed, the strength of such calibration is to reproduce as well as possible the present state of endpoints in response to the current soil contamination. But the extrapolation over the range of calibration is difficult. In order to estimate the future of areas that are soon to be contaminated several ecotoxicological studies employed a space for time approach. This approach may be reliable for nearby areas; however, studies suggest that ecosystem responses to soil contamination may vary depending on regional weather conditions (Li et al., 2017; Moe et al., 2013; Tobor-Kapton et al., 2006). Therefore, generalizing response functions to soil contamination may be unreliable over large area.

The second approach is better suited for prospective studies as laboratory studies enable the use of higher concentrations of contaminants to investigate endpoints responses. However, this requires to conduct many experimental studies taking into account the multiplicity of co-factors (soil pH, texture, climate...). Moreover, the processes studied in micro or mesocosms for calibration functions purposes may not reflect

the ecosystem's responses or the large-scale processes being modeled. For instance, it has been shown that soil contamination may affect both the microbial efficiency and the microbial amount. The outcomes of these two effects may vary for key long-term processes in LSMs, such as soil CO<sub>2</sub> emissions and SOC concentrations. However, as the explicit representation of microbial biomass has not yet been implemented in LSMs, model-specific adaptations of response functions to soil contamination will be required. More generally, the explicit representations of small scale processes into LSMs is still under investigation (Fisher and Koven, 2020).

#### 4.2. Regional analysis of soil contamination

Our study was enabled by the extensive and accurate soil survey's carried out by the JRC, providing soil data (including SOC, pH, CEC, CaCO<sub>3</sub>, Cu) with a precision close to 0.1° across the entire European Union (Ballabio et al., 2019, 2016). This allowed us to confront several LSMs bias to all soil properties across many grid points and at one of the most precise scales available for LSMs (0.5°). However, the resolution for geochemical and contaminant variations is coarse (Anav et al., 2013; Tóth et al., 2016). The mapping of soil Cu at 0.5° used here limits the hot spots of Cu concentration, with only 1/1570 grid points with Cu > 100 mgCu·kg<sup>-1</sup> and 13/1570 grid points with Cu > 50 mgCu·kg<sup>-1</sup>. The results presented here also relate to more diffuse contamination, limited to areas of at least 0.5° and a few decades to hundred mgCu·kg<sup>-1</sup>. In contrast, (Ballabio et al., 2018) soil survey study found Cu concentrations > 100 mgCu·kg<sup>-1</sup> in 1.1 % of the samples with vineyards exhibiting a Cu mean close to 50 mgCu·kg<sup>-1</sup>. Previous study on laboratory incubation found a general decrease in soil Rh with an increase in soil Cu contamination despite an increase in soil Rh at limited Cu concentration for freshly contaminated soils (Sereni et al., 2021).

Due to the small number of grids point available at high concentrations, it is difficult to establish the robustness of the observed decrease trend. Moreover, our study was restricted to the European scale, while the response of ecosystems to external disruption may significantly differ across various biomes (Beaumelle et al., 2021; Bowler et al., 2020; Clements and Rohr, 2009). With growing interest in soil Rh, databases at large scale and coarse resolutions are regularly published based on different aggregation procedures. Thus, it could enhance our analysis if we compared coarser and broader databases established worldwide (Bond-Lamberty et al., 2020; Jian et al., 2021).

Moreover, we focused on the soil Cu concentration as a model for soil contamination because Cu is widely used in agricultural sectors and well-studied. However, soil contamination rarely occurs with a single contaminant. Indeed, atmospheric deposition from industries or transports is often a mixture of heavy metals while agricultural fungicides

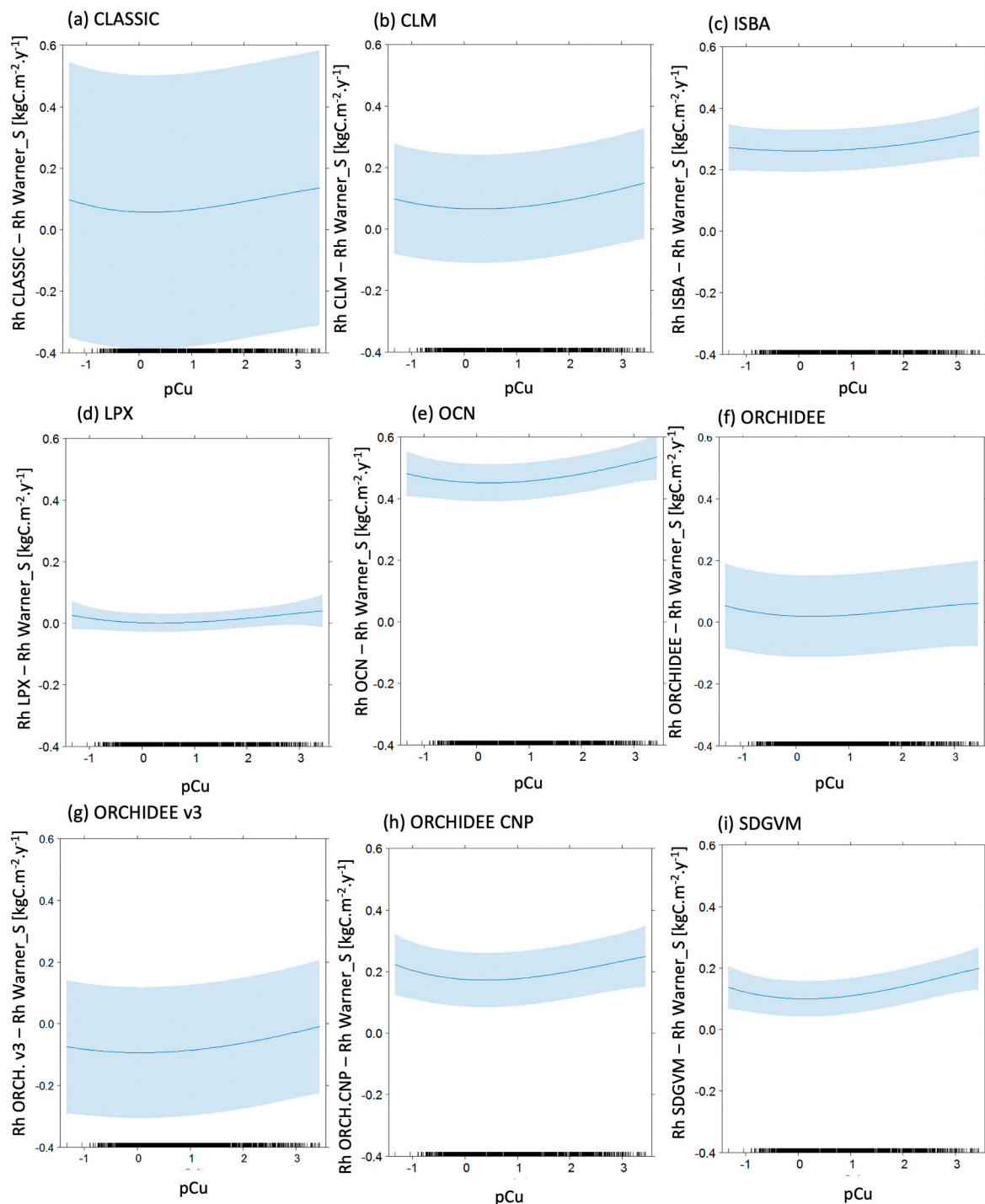


**Fig. 6.** Partial pCu effects plots for the differences between models and Warner\_S's Rh. Results are only shown for models where pCu was selected through step AIC using set F of initial predictors. (a) CLASSIC model, (b) CLM model, (c) ISBA, (d) LPX, (e) OCN, (f) ORCHIDEE, (g) ORCHIDEE v3, (h) ORCHIDEE CNP, (i) SDGVM.

and pesticides also contain organic components. For instance, in Europe, (Tóth et al., 2016) found that, Cu concentrations were highly correlated to Co, Cr, Mn, Ni and Sb concentrations. The impact of multiple contaminations on soil functions is still poorly documented. In some cases, soil fauna adaptation to one contaminant may limit the effects of the others, while in other cases stress combination can escalate the effects on fauna or functions (Rillig et al., 2019; Wakelin et al., 2014; Zeng et al., 2017). Finally, contaminants have different sources and environmental mobilities so that the scale of contamination diffusion may vary. Hence, if our study emphasized the significance of Cu contamination for Rh modelling at 0.5°, dominant contaminant may differ with spatial

resolution. However, as it arise 1) from the Tóth et al. (2016) study that soil contaminants behave by pools and 2) from our study that Cu concentration is correlated with models bias at the 0.5° scale, these two points made Cu a good candidate to proxy soil contamination at this scale and to account for it in LSM. However, further research is needed to understand co-pollutants and the mechanisms of Rh changes to help design policies to address the impact of soil contamination on soil CO<sub>2</sub>.

#### 4.3. Uncertainties in Rh estimations

In this study we observed differences between Warner\_S's Rh

observation's derived products and Hashimoto et al. (2015)'s Rh observation derived products. These two products are based on different statistical mapping at the worldwide scale based on few thousand points. Thus, the predictors conserved to explain Rh bias by comparison of each of the two observation products differ. The strong dependency of Hashimoto's Rh on climate factors might be explained by its construction involving a semi empirical function of temperature and rainfall (Hashimoto et al., 2015). In contrast, Warner\_S's Rh is constructed utilizing a random forest algorithm and is explained by several pedological factors even if the factors for the published data base construction were restricted to temperature, rainfall (annual mean and mean from November to January) and enhanced vegetation indexes. Over Europe, (Ballabio et al., 2018) found that there was a correlation between soil Cu concentration and spring temperature and rainfall. More precisely, Cu concentration was high in areas with high levels of humidity and heat, especially in vineyards where fungicides were frequently applied to combat downy mildew. Thus, with the inclusion of enhanced vegetation index Warner\_S's Rh random forests algorithm might take into account predictors as CaCO<sub>3</sub>, clay, pH or Cu. Due to their statistical derivations, the observation products differ in their strength of Rh variability reproduction. Therefore, to limit false positives and negatives resulting from the methods of deriving observation products, several products were analyzed in the residual analysis of the model.

Among the 11 models analyzed, the bias towards observations varies largely in mean or median, with most models mean and median very close to the observed mean or median while CLASSIC or OCN twice larges. CLASSIC model differences can be explained by the initial resolution of the model that was provided at the 2.8° × 2.8° scale, limiting the spatial variability as well than missing some region such as Brittany. Besides, models differ in the process they include such as fire management, explicit N processes ... (Friedlingstein et al., 2020) that plays a role in C cycle and Rh estimations. However, the models also differ in the conceptualization of soil C cycle and parametrization. Also, the direct extraction of key processes that have to be represented to limit bias is not possible. The parameters selection conducted in the present study does not allow to assess which exact processes involved in Rh is not well modeled but it allows the identification of environmental parameters for which the response is not well accounted for.

#### 4.4. Implications for soil management

Numerous policies aim at increasing the C stocks in soils (European Commission Directorate-General for Research and Innovation et al., 2020), with one of the most efficient way being to use organic fertilizers. For instance, sewage water or pig slurry are often used for soil amendment but are also rich in heavy metals such as Cu. Regular amendment with organic fertilizers can thus affect both soil organic C and soil Cu content (Denaix et al., 2013; Jensen et al., 2016; Parat et al., 2007; Smolders et al., 2012), but also pH leading to supplementary uncertainties (Laurent et al., 2020). Here, we showed that the soil Cu concentration might affect soil Rh but that it is not accounted properly in current soil model used to estimate the effect of land use change or climate change on soil C emissions. Given that soil Rh represents one of the main soil-atmosphere C flux, our study argues that a better understanding and representation of the effect of soil Cu contamination on soil Rh is of major interest for soil C storage policies.

## 5. Conclusion

The comparison of Rh to soil Cu concentration databases revealed that soil Cu concentration was a relevant predictor for Rh defined at 0.5° scale across Europe. Indeed, limited significant effect of Cu was found by comparison to Hashimoto's Rh whereas significant effect of Cu was found by comparison to Warner\_S's Rh, that also show coarser variations at the regional scale. Our results also show that both total Cu and free Cu were relevant predictors of Rh. Although there was little accuracy

improvement using free Cu. The analysis conducted on 11 LSMs indicated that in most cases, Cu may account for the residuals. Cu (expressed as a total content or as a bioavailable pool) was found significant with an effect of the same order of magnitude than the other soil factors in 24 of the 42 studied cases. For both total Cu and free Cu, soil ΔRh was found to globally decrease with an increase in soil Cu. In some cases, ΔRh increases for moderate and/or very large Cu concentrations. However, the Cu concentration with inversion from an increase to a decrease in soil ΔRh largely varied among the models and the observations considered. None of these LSMs accounted for Cu. Also, the various responses we observed could be attributed to the varying calibration of response functions to co-varying parameters such as pH or climate.

## CRedit authorship contribution statement

**Laura Sereni:** Writing – review & editing, Writing – original draft, Methodology, Investigation, Formal analysis, Data curation. **Isabelle Lamy:** Writing – review & editing, Supervision, Methodology, Funding acquisition, Conceptualization. **Bertrand Guenet:** Writing – review & editing, Supervision, Methodology, Funding acquisition, Conceptualization.

## Declaration of competing interest

Authors have no competing interests to declare.

## Acknowledgements

Parts of this study were financially supported by the Labex BASC through the Connexion project. LS thanks the Ecole Normale Supérieure (ENS) for funding her PhD. We thank all people and institutions within the “Trends and drivers of the regional-scale sources and sinks of carbon dioxide” (TRENDY) modelling groups who contributed to the data used in this study. We thank Philipp Peylin for his help with TRENDY output processing.

## Appendix A. Supplementary data

Supplementary data to this article can be found online at <https://doi.org/10.1016/j.scitotenv.2024.177574>.

## Data availability

The data that support the findings of this study are available from the corresponding author upon reasonable request.

## References

- Alloway, B.J., 2013. Sources of heavy metals and metalloids in soils. In: Alloway, B.J. (Ed.), *Heavy Metals in Soils: Trace Metals and Metalloids in Soils and Their Bioavailability*. Springer Netherlands, Dordrecht, pp. 11–50. [https://doi.org/10.1007/978-94-007-4470-7\\_2](https://doi.org/10.1007/978-94-007-4470-7_2).
- Anav, A., Friedlingstein, P., Kidston, M., Bopp, L., Ciais, P., Cox, P., Jones, C., Jung, M., Myneni, R., Zhu, Z., 2013. Evaluating the land and ocean components of the global carbon cycle in the CMIP5 earth system models. *J. Climate* 26, 6801–6843. <https://doi.org/10.1175/JCLI-D-12-00417.1>.
- Bååth, E., 1989. Effects of heavy metals in soil on microbial processes and populations (a review). *Water Air Soil Pollut.* 47, 335–379. <https://doi.org/10.1007/BF00279331>.
- Ballabio, C., Panagos, P., Montanarella, L., 2016. Mapping topsoil physical properties at European scale using the LUCAS database. *Geoderma*. <https://doi.org/10.1016/j.geoderma.2015.07.006>.
- Ballabio, C., Panagos, P., Lugato, E., Huang, J.H., Orgiazzi, A., Jones, A., Fernández-Ugalde, O., Borrelli, P., Montanarella, L., 2018. Copper distribution in European topsoils: an assessment based on LUCAS soil survey. *Sci. Total Environ.* 636, 282–298. <https://doi.org/10.1016/j.scitotenv.2018.04.268>.
- Ballabio, C., Lugato, E., Fernández-Ugalde, O., Orgiazzi, A., Jones, A., Borrelli, P., Montanarella, L., Panagos, P., 2019. Mapping LUCAS topsoil chemical properties at European scale using Gaussian process regression. *Geoderma*. <https://doi.org/10.1016/j.geoderma.2019.113912>.
- Beaumelle, L., Thouvenot, L., Hines, J., Jochum, M., Eisenhauer, N., Phillips, H.R.P., 2021. Soil fauna diversity and chemical stressors: a review of knowledge gaps and

- roadmap for future research. *Ecography* 44, 845–859. <https://doi.org/10.1111/ecog.05627>.
- Blyth, E.M., Arora, V.K., Clark, D.B., Dadson, S.J., De Kauwe, M.G., Lawrence, D.M., Melton, J.R., Pongratz, J., Turton, R.H., Yoshimura, K., Yuan, H., 2021. Advances in land surface modelling. *Curr. Clim. Chang. Rep.* 7, 45–71. <https://doi.org/10.1007/s40641-021-00171-5>.
- Bond-Lamberty, B., Christianson, D.S., Malhotra, A., Pennington, S.C., Sih, D., AghaKouchak, A., Anjileli, H., Altaf Arain, M., Armesto, J.J., Ashraf, S., Ataka, M., Baldocchi, D., Andrew Black, T., Buchmann, N., Carbone, M.S., Chang, S.C., Crill, P., Curtis, P.S., Davidson, E.A., Desai, A.R., Drake, J.E., El-Madany, T.S., Gavazzi, M., Göres, C.M., Gough, C.M., Goulden, M., Gregg, J., Gutiérrez del Arroyo, O., He, J.S., Hirano, T., Hoppel, A., Hughes, H., Järveoja, J., Jassal, R., Jian, J., Kan, H., Kaye, J., Kominami, Y., Liang, N., Lipson, D., Macdonald, C.A., Maseyk, K., Mathes, K., Mauritz, M., Mayes, M.A., McNulty, S., Miao, G., Migliavacca, M., Miller, S., Miniati, C.F., Nietz, J.G., Nilsson, M.B., Noormets, A., Noruzzi, H., O'Connell, C.S., Osborne, B., Oyonaite, C., Pang, Z., Peichl, M., Pendall, E., Perez-Quezada, J.F., Phillips, C.L., Phillips, R.P., Raich, J.W., Renchon, A.A., RUEHR, N.K., Sánchez-Cañete, E.P., Saunders, M., Savage, K.E., Schrumpp, M., Scott, R.L., Seibt, U., Silver, W.L., Sun, W., Szutu, D., Takagi, K., Takagi, M., Teramoto, M., Tjoelker, M.G., Trumbore, S., Ueyama, M., Vargas, R., Varner, R.K., Verfaillie, J., Vogel, C., Wang, J., Winston, G., Wood, T.E., Wu, J., Wutzler, T., Zeng, J., Zha, T., Zhang, Q., Zou, J., 2020. COSORE: a community database for continuous soil respiration and other soil-atmosphere greenhouse gas flux data. *Glob. Chang. Biol.* 26, 7268–7283. <https://doi.org/10.1111/gcb.15353>.
- Bowler, D.E., Bjorkman, A.D., Dornelas, M., Myers-Smith, I.H., Navarro, L.M., Niamir, A., Supp, S.R., Waldock, C., Winter, M., Vellend, M., Blowes, S.A., Böhnning-Gaese, K., Bruehlheide, H., Elahi, R., Antão, L.H., Hines, J., Isbell, F., Jones, H.P., Magurran, A. E., Cabral, J.S., Bates, A.E., 2020. Mapping human pressures on biodiversity across the planet uncovers anthropogenic threat complexes. *People and Nature* 2, 380–394. <https://doi.org/10.1002/pan3.10071>.
- Cao, H., Chang, A.C., Page, A.L., 1984. Heavy Metal Contents of Sludge-Treated Soils as Determined by Three Extraction Procedures Been Recommended as Availability Indices of Metals in Soil (Lagerwerff, 1971; John et al., 1972; Symeonides Reisenauer, 1982). Under experimental conditions, pp. 2–4.
- Clements, W.H., Rohr, J.R., 2009. Community responses to contaminants: using basic ecological principles to predict ecotoxicological effects. *Environ. Toxicol. Chem.* 28, 1789–1800. <https://doi.org/10.1897/09-140.1>.
- Cox, P.M., Betts, R.A., Jones, C.D., Spall, S.A., Totterdell, I.J., 2000. Acceleration of global warming due to carbon-cycle feedbacks in a coupled climate model. *Nature* 408, 184–187. <https://doi.org/10.1038/35041539>.
- de Brogniez, D., Ballabio, C., Stevens, A., Jones, R.J.A., Montanarella, L., van Wesemael, B., 2015. A map of the topsoil organic carbon content of Europe generated by a generalized additive model. *Eur. J. Soil Sci.* <https://doi.org/10.1111/ejss.12193>.
- Delire, C., Séférian, R., Decharme, B., Alkama, R., Calvet, J.C., Carrer, D., Gibelin, A.L., Joetzjer, E., Morel, X., Rocher, M., Tzanos, D., 2020. The global land carbon cycle simulated with ISBA-CTRIP: improvements over the last decade. *Journal of Advances in Modeling Earth Systems.* <https://doi.org/10.1029/2019MS001886>.
- Denaix, L., Nguyen, C., Heroult, J., Parat, C., Lespes, G., Potin-Gautier, M., Coudure, R., Dauguet, S., 2013. Quantification of Trace Elements Fluxes (As, Cd, Cu, Pb, Zn) Into Agricultural Fields Amended With Pig Slurry.
- Doetterl, S., Stevens, A., Six, J., Merckx, R., Van Oost, K., Casanova Pinto, M., Casanova-Katny, A., Muñoz, C., Boudin, M., Zagal Venegas, E., Boeckx, P., 2015. Soil carbon storage controlled by interactions between geochemistry and climate. *Nat. Geosci.* <https://doi.org/10.1038/ngeo2516>.
- European Commission Directorate-General for Research and Innovation, Veerman, C., Pinto Correia, T., Bastioli, C., Biro, B., Bouma, J., Cienciala, E., Emmett, B., Frison, E. A., Grand, A., Hristov, L., Kriauciūnienė, Z., Pogrzeba, M., Soussana, J.-F., Vela, C.O., Wittkowski, R., 2020. Caring for Soil is Caring for Life: Ensure 75% of Soils are Healthy by 2030 for Food, People, Nature and Climate: Report of the Mission Board for Soil Health and Food. Publications Office of the European Union.
- Fisher, R.A., Koven, C.D., 2020. Perspectives on the future of land surface models and the challenges of representing complex terrestrial systems. *Journal of Advances in Modeling Earth Systems* 12. <https://doi.org/10.1029/2018MS001453>.
- Friedlingstein, P., Cox, P., Betts, R., Bopp, L., von Bloh, W., Brovkin, V., Cadule, P., Doney, S., Eby, M., Fung, I., Bala, G., John, J., Jones, C., Joos, F., Kato, T., Kawamiya, M., Knorr, W., Lindsay, K., Matthews, H.D., Raddatz, T., Rayner, P., Reick, C., Roeckner, E., Schnitzler, K.G., Schnur, R., Strassmann, K., Weaver, A.J., Yoshikawa, C., Zeng, N., 2006. Climate-carbon cycle feedback analysis: results from the C4MIP model intercomparison. *J. Climate* 19, 3337–3353. <https://doi.org/10.1175/JCLI3800.1>.
- Friedlingstein, P., O'Sullivan, M., Jones, M.W., Andrew, R.M., Hauck, J., Olsen, A., Peters, G.P., Peters, W., Pongratz, J., Sitch, S., Le Quééré, C., Canadell, J.G., Ciais, P., Jackson, R.B., Alin, S., Aragão, L.E.O.C., Arneeth, A., Arora, V., Bates, N.R., Becker, M., Benoit-Cattin, A., Bittig, H.C., Bopp, L., Bultan, S., Chandra, N., Chevallier, F., Chini, L.P., Evans, W., Florentie, L., Forster, P.M., Gasser, T., Gehlen, M., Gilfillan, D., Gkriztilis, T., Gregor, L., Gruber, N., Harris, I., Hartung, K., Haverd, V., Houghton, R.A., Ilyina, T., Jain, A.K., Joetzjer, E., Kadono, K., Kato, E., Kitidis, V., Korsbakken, J.I., Landschützer, P., Lefèvre, N., Lenton, A., Lienert, S., Liu, Z., Lombardozzi, D., Marland, G., Metzl, N., Munro, D.R., Nabel, J.E.M.S., Nakaoka, S.-I., Niwa, Y., O'Brien, K., Ono, T., Palmer, P.I., Pierrot, D., Poulter, B., Resplandy, L., Robertson, E., Rödenbeck, C., Schwinger, J., Séférian, R., Skjelvan, I., Smith, A.J.P., Sutton, A.J., Tanhua, T., Tans, P.P., Tian, H., Tilbrook, B., Van Der Werf, G., Vuichard, N., Walker, A.P., Wanninkhof, R., Watson, A.J., Willis, D., Wiltshire, A.J., Yuan, W., Yue, X., Zaehle, S., 2020. Global carbon budget 2020. *Earth Syst. Sci. Data* 12, 3269–3340. <https://doi.org/10.5194/essd-12-3269-2020>.
- Giller, K.E., Witter, E., Mcgrath, S.P., 1998. Toxicity of heavy metals to microorganisms and microbial processes in agricultural soils: a review. *Soil Biol. Biochem.* 30, 1389–1414. [https://doi.org/10.1016/S0038-0717\(97\)00270-8](https://doi.org/10.1016/S0038-0717(97)00270-8).
- Giller, K.E., Witter, E., McGrath, S.P., 2009. Heavy metals and soil microbes. *Soil Biol. Biochem.* 41, 2031–2037. <https://doi.org/10.1016/j.soilbio.2009.04.026>.
- Goll, D.S., Vuichard, N., Maignan, F., Jorner-Puig, A., Sardans, J., Violette, A., Peng, S., Sun, Y., Kvakic, M., Guimberteau, M., Guenet, B., Zaehle, S., Penuelas, J., Janssens, I., Ciais, P., 2017. A representation of the phosphorus cycle for ORCHIDEE (revision 4520). *Geosci. Model Dev.* 10, 3745–3770. <https://doi.org/10.5194/gmd-10-3745-2017>.
- Hashimoto, S., Carvalhais, N., Ito, A., Migliavacca, M., Nishina, K., Reichstein, M., 2015. Global spatiotemporal distribution of soil respiration modeled using a global database. *Biogeosciences* 12, 4121–4132. <https://doi.org/10.5194/bg-12-4121-2015>.
- Huntzinger, D.N., Michalak, A.M., Schwalm, C., Ciais, P., King, A.W., Fang, Y., Schaefer, K., Wei, Y., Cook, R.B., Fisher, J.B., Hayes, D., Huang, M., Ito, A., Jain, A. K., Lei, H., Lu, C., Maignan, F., Mao, J., Parazoo, N., Peng, S., Poulter, B., Ricciuto, D., Shi, X., Tian, H., Wang, W., Zeng, N., Zhao, F., 2017. Uncertainty in the response of terrestrial carbon sink to environmental drivers undermines carbon-climate feedback predictions. *Sci. Rep.* 7. <https://doi.org/10.1038/s41598-017-03818-2>.
- Jensen, J., Larsen, M.M., Bak, J., 2016. National monitoring study in Denmark finds increased and critical levels of copper and zinc in arable soils fertilized with pig slurry. *Environ. Pollut.* 214, 334–340. <https://doi.org/10.1016/j.envpol.2016.03.034>.
- Jian, J., Vargas, R., Anderson-Teixeira, K., Stell, E., Herrmann, V., Horn, M., Kholod, N., Manzoni, J., Marchesi, R., Paredes, D., Bond-Lamberty, B., 2021. A restructured and updated global soil respiration database (SRDB-V5). *Earth System Science Data* 13, 255–267. <https://doi.org/10.5194/essd-13-255-2021>.
- Konings, A.G., Bloom, A.A., Liu, J., Parazoo, N.C., Schimel, D.S., Bowman, K.W., 2019. Global Satellite-driven Estimates of Heterotrophic Respiration, pp. 2269–2284.
- Krinner, G., Viovy, N., de Noblet-Ducoudré, N., Ogée, J., Polcher, J., Friedlingstein, P., Ciais, P., Sitch, S., Prentice, I.C., 2005. A dynamic global vegetation model for studies of the coupled atmosphere-biosphere system. *Global Biogeochem. Cycles.* <https://doi.org/10.1029/2003GB002199>.
- Lanno, R., Wells, J., Conder, J., Bradham, K., Basta, N., 2004. The bioavailability of chemicals in soil for earthworms. In: *Ecotoxicology and Environmental Safety.* <https://doi.org/10.1016/j.ecoenv.2003.08.014>.
- Laurent, C., Bravin, M.N., Crouzet, O., Pelosi, C., Tillard, E., Lecomte, P., Lamy, I., 2020. Increased soil pH and dissolved organic matter after a decade of organic fertilizer application mitigates copper and zinc availability despite contamination. *Soil. Total Environ.* 709, 135927. <https://doi.org/10.1016/j.scitotenv.2019.135927>.
- Lawrence, D.M., Fisher, R.A., Koven, C.D., Oleson, K.W., Swenson, S.C., Bonan, G., Collier, N., Ghimire, B., van Kampenhou, L., Kennedy, D., Kluzek, E., Lawrence, P.J., Li, F., Li, H., Lombardozzi, D., Riley, W.J., Sacks, W.J., Shi, M., Vertenstein, M., Wieder, W.R., Xu, C., Ali, A.A., Badger, A.M., Bisht, G., van den Broeke, M., Brunke, M.A., Burns, S.P., Buzan, J., Clark, M., Craig, A., Dahlin, K., Drewniak, B., Fisher, J.B., Flanner, M., Fox, A.M., Gentine, P., Hoffman, F., Keppel-Aleks, G., Knox, R., Kumar, S., Lenaerts, J., Leung, L.R., Lipscomb, W.H., Lu, Y., Pandey, A., Pelletier, J.D., Perket, J., Randerson, J.T., Ricciuto, D.M., Sanderson, B.M., Slater, A., Subin, Z.M., Tang, J., Thomas, R.Q., Val Martin, M., Zeng, X., 2019. The community land model version 5: description of New features, benchmarking, and impact of forcing uncertainty. *Journal of Advances in Modeling Earth Systems.* <https://doi.org/10.1029/2018MS001583>.
- Li, J., Liu, Y.R., Cui, L.J., Hu, H.W., Wang, J.T., He, J.Z., 2017. Copper pollution increases the resistance of soil archaeal community to changes in water regime. *Microb. Ecol.* <https://doi.org/10.1007/s00248-017-0992-0>.
- Lienert, S., Joos, F., 2018. A Bayesian ensemble data assimilation to constrain model parameters and land-use carbon emissions. *Biogeosciences.* <https://doi.org/10.5194/bg-15-2909-2018>.
- Lofts, S., Criel, P., Janssen, C.R., Lock, K., McGrath, S.P., Oorts, K., Rooney, C.P., Smolders, E., Spurgeon, D.J., Svendsen, C., Van Eeckhout, H., Zhao, F.Z., 2013. Modelling the effects of copper on soil organisms and processes using the free ion approach: towards a multi-species toxicity model. *Environ. Pollut.* 178, 244–253. <https://doi.org/10.1016/j.envpol.2013.03.015>.
- McBride, M., Sauvé, S., Hendershot, W., 1997. Solubility control of Cu, Zn, Cd and Pb in contaminated soils. *Eur. J. Soil Sci.* 48, 337–346. <https://doi.org/10.1111/j.1365-2389.1997.tb00554.x>.
- Meiyappan, P., Jain, A.K., House, J.I., 2015. Increased influence of nitrogen limitation on CO2 emissions from future land use and land use change. *Global Biogeochem. Cycles.* <https://doi.org/10.1002/2015GB005086>.
- Melton, J.R., Arora, V.K., Wisernig-Cojoc, E., Seiler, C., Fortier, M., Chan, E., Teckentrup, L., 2020. CLASSIC v1.0: the open-source community successor to the Canadian Land Surface Scheme (CLASS) and the Canadian Terrestrial Ecosystem Model (CTEM)-part 1: model framework and site-level performance. *Geosci. Model Dev.* 13, 2825–2850. <https://doi.org/10.5194/gmd-13-2825-2020>.
- Mitchell, T.D., Carter, T.R., Jones, P.D., Hulme, M., New, M., 2004. A comprehensive set of high-resolution grids of monthly climate for Europe and the globe: the observed record (1901–2000) and 16 scenarios (2001–2100). *Geography* 55, 30.
- Moe, S.J., De Schampelaere, K., Clements, W.H., Sorensen, M.T., Van den Brink, P.J., Liess, M., 2013. Combined and interactive effects of global climate change and toxicants on populations and communities. *Environ. Toxicol. Chem.* 32, 49–61. <https://doi.org/10.1002/etc.2045>.
- Official Journal of the European Union, 2018. Official Journal of the European Union - Cu Regulation [WWW Document]. URL. [https://eur-lex.europa.eu/eli/reg\\_impl/2018/1039/oj](https://eur-lex.europa.eu/eli/reg_impl/2018/1039/oj) (accessed 3.15.24).

- Panagos, P., Ballabio, C., Lugato, E., Jones, A., Borrelli, P., Scarpa, S., Orgiazzi, A., Montanarella, L., 2018. Potential sources of anthropogenic copper inputs to European agricultural soils. *Sustainability (Switzerland)* 10, 2–18. <https://doi.org/10.3390/su10072380>.
- Parat, C., Denaix, L., Lévêque, J., Chaussod, R., Andreux, F., 2007. The organic carbon derived from sewage sludge as a key parameter determining the fate of trace metals. *Chemosphere* 69, 636–643. <https://doi.org/10.1016/j.chemosphere.2007.02.069>.
- Parker, D.R., Pedler, J.F., Ahnstrom, Z.A.S., Resketo, M., 2001. Reevaluating the free-ion activity model of trace metal toxicity toward higher plants: experimental evidence with copper and zinc. *Environ. Toxicol. Chem.* <https://doi.org/10.1002/etc.5620200426>.
- Pauget, B., Gimbert, F., Scheifler, R., Coeurdassier, M., De Vaufléury, A., 2012. Soil parameters are key factors to predict metal bioavailability to snails based on chemical extractant data. *Sci. Total Environ.* <https://doi.org/10.1016/j.scitotenv.2012.05.048>.
- Pinheiro, J., DebRoy, Saikat, Sarkar, D., Heisterkamp, S., Van Wiligen, B., Ranke, J., Bayes, Douglas, 2023. *nlme: Linear and Nonlinear Mixed Effects Models*.
- R Core Team, 2018. R Software: Version 3.5.1. R Foundation for Statistical Computing. <https://doi.org/10.1007/978-3-540-74686-7>.
- Rillig, M.C., Ryo, M., Lehmann, A., Aguilar-Trigueros, C.A., Buchert, S., Wulf, A., Iwasaki, A., Roy, J., Yang, G., 2019. The role of multiple global change factors in driving soil functions and microbial biodiversity. *Science* 366, 886–890. <https://doi.org/10.1126/science.aay2832>.
- Seiler, C., Melton, J.R., Arora, V.K., Wang, L., 2021. CLASSIC v1.0: the open-source community successor to the Canadian Land Surface Scheme (CLASS) and the Canadian Terrestrial Ecosystem Model (CTEM) - part 2: global benchmarking. *Geosci. Model Dev.* <https://doi.org/10.5194/gmd-14-2371-2021>.
- Sereni, L., Guenet, B., Lamy, I., 2021. Does copper contamination affect soil CO<sub>2</sub> emissions? A literature review. *Front. Environ. Sci.* 9, 29. <https://doi.org/10.3389/fenvs.2021.585677>.
- Sitch, S., Friedlingstein, P., Gruber, N., Jones, S.D., Murray-Tortarolo, G., Ahlström, A., Doney, S.C., Graven, H., Heinze, C., Huntingford, C., Levis, S., Levy, P.E., Lomas, M., Poulter, B., Viovy, N., Zaehle, S., Zeng, N., Arneeth, A., Bonan, G., Bopp, L., Canadell, J.G., Chevallier, F., Ciais, P., Ellis, R., Gloor, M., Peylin, P., Piao, S.L., Le Quéré, C., Smith, B., Zhu, Z., Myneni, R., 2015. Recent trends and drivers of regional sources and sinks of carbon dioxide. *Biogeosciences* 12, 653–679. <https://doi.org/10.5194/bg-12-653-2015>.
- Smith, W.K., Reed, S.C., Cleveland, C.C., Ballantyne, A.P., Anderegg, W.R.L., Wieder, W. R., Liu, Y.Y., Running, S.W., 2016. Large divergence of satellite and earth system model estimates of global terrestrial CO<sub>2</sub> fertilization. *Nat. Clim. Chang.* 6, 306–310. <https://doi.org/10.1038/nclimate2879>.
- Smolders, E., Oorts, K., Lombi, E., Schoeters, I., Ma, Y., Zrna, S., McLaughlin, M.J., 2012. The availability of copper in soils historically amended with sewage sludge, manure, and compost. *J. Environ. Qual.* <https://doi.org/10.2134/jeq2011.0317>.
- Smorkalov, I.A., Vorobeichik, E.L., 2011. Soil respiration of forest ecosystems in gradients of environmental pollution by emissions from copper smelters. *Russ. J. Ecol.* 42, 464–470. <https://doi.org/10.1134/S1067413611060166>.
- Steinnes, E., Allen, R.O., Petersen, H.M., Rambøll, J.P., Varskog, P., 1997. Evidence of large scale heavy-metal contamination of natural surface soils in Norway from long-range atmospheric transport. *Sci. Total Environ.* 205, 255–266. [https://doi.org/10.1016/S0048-9697\(97\)00209-X](https://doi.org/10.1016/S0048-9697(97)00209-X).
- Thakali, S., Allen, H.E., Di Toro, D.M., Ponizovsky, A.A., Rodney, C.P., Zhao, F.J., McGrath, S.P., 2006. A Terrestrial Biotic Ligand Model. 1. Development and application to Cu and Ni toxicities to barley root elongation in soils. *Environ. Sci. Tech.* 40, 7085–7093. <https://doi.org/10.1021/es061171s>.
- Thornton, I., Webb, J.S., 1980. Trace elements in soils and plants. In: *Food Chains and Human Nutrition*. [https://doi.org/10.1007/978-94-011-7336-0\\_12](https://doi.org/10.1007/978-94-011-7336-0_12).
- Tipping, E., Rieuwerts, J., Pan, G., Ashmore, M.R., Lofts, S., Hill, M.T.R., Farago, M.E., Thornton, I., 2003. The solid-solution partitioning of heavy metals (Cu, Zn, Cd, Pb) in upland soils of England and Wales. *Environ. Pollut.* 125, 213–225. [https://doi.org/10.1016/S0269-7491\(03\)00058-7](https://doi.org/10.1016/S0269-7491(03)00058-7).
- Tobor-Kaplon, M.A., Bloem, J., De Ruiter, P.C., 2006. Functional stability of microbial communities from long-term stressed soils to additional disturbance. *Environ. Toxicol. Chem.* <https://doi.org/10.1897/05-398R1.1>.
- Tóth, G., Hermann, T., Szatmári, G., Pásztor, L., 2016. Maps of heavy metals in the soils of the European Union and proposed priority areas for detailed assessment. *Sci. Total Environ.* 565, 1054–1062. <https://doi.org/10.1016/j.scitotenv.2016.05.115>.
- Vargas, R., Carbone, M.S., Reichstein, M., Baldocchi, D.D., 2011. Frontiers and challenges in soil respiration research: from measurements to model-data integration. *Biogeochemistry* 102, 1–13. <https://doi.org/10.1007/S10533-010-9462-1/FIGURES/5>.
- Vuichard, N., Messina, P., Luysaert, S., Guenet, B., Zaehle, S., Ghattas, J., Bastrikov, V., Peylin, P., 2019. Accounting for Carbon and Nitrogen interactions in the Global Terrestrial Ecosystem Model ORCHIDEE (trunk version, rev 4999): multi-scale evaluation of gross primary production. *Geoscientific Model Development Discussions* 12, 4751–4779. <https://doi.org/10.5194/gmd-2018-261>.
- Wakelin, S., Gerard, E., Black, A., Hamonts, K., Condrón, L., Yuan, T., Van Nostrand, J., Zhou, J., O'Callaghan, M., 2014. Mechanisms of pollution induced community tolerance in a soil microbial community exposed to Cu. *Environ. Pollut.* 190, 1–9. <https://doi.org/10.1016/j.envpol.2014.03.008>.
- Walker, A.P., Quaipe, T., van Bodegom, P.M., De Kauwe, M.G., Keenan, T.F., Joiner, J., Lomas, M.R., MacBean, N., Xu, C., Yang, X., Woodward, F.I., 2017. The impact of alternative trait-scaling hypotheses for the maximum photosynthetic carboxylation rate (V<sub>cmax</sub>) on global gross primary production. *New Phytol.* <https://doi.org/10.1111/nph.14623>.
- Warner, D.L., Bond-Lamberty, B., Jian, J., Stell, E., Vargas, R., 2019. Spatial predictions and associated uncertainty of annual soil respiration at the global scale. *Global Biogeochem. Cycles* 33, 1733–1745. <https://doi.org/10.1029/2019GB006264>.
- Yang, Y., Campbell, C.D., Clark, L., Cameron, C.M., Paterson, E., 2006. Microbial indicators of heavy metal contamination in urban and rural soils. *Chemosphere* 63, 1942–1952. <https://doi.org/10.1016/j.chemosphere.2005.10.009>.
- Yao, Y., Ciais, P., Viovy, N., Li, W., Cresto-Aleina, F., Yang, H., Joetzer, E., Bond-Lamberty, B., 2021. A data-driven global soil heterotrophic respiration dataset and the drivers of its inter-annual variability. *Global Biogeochem. Cycles*. <https://doi.org/10.1029/2020GB006918>.
- Yuan, C., Huang, T., Zhao, X., Zhao, Y., 2020. Numerical models of subsurface flow constructed wetlands: review and future development. *Sustainability (Switzerland)* 12, 1–16. <https://doi.org/10.3390/SU12083498>.
- Zaehle, S., Friend, A., 2010. Carbon and nitrogen cycle dynamics in the O-CN land surface model: 1. Model description, site-scale evaluation, and sensitivity to parameter estimates. *Global Biogeochem. Cycles* 24. <https://doi.org/10.1029/2009GB003521>.
- Zeng, S., Li, J., Wei, D., Ma, Y., 2017. A new model integrating short- and long-term aging of copper added to soils. *PLoS One* 12, 19–24. <https://doi.org/10.1371/journal.pone.0182944>.